View metadata, citation and similar papers at core.ac.uk

brought to you by CORE

provided by Elsevier - Publisher Connector

Available online at www.sciencedirect.com

SCIENCE DIRECT®

Vision Research 45 (2005) 2145–2160

Vision Research

www.elsevier.com/locate/visres

Detection of symmetry and anti-symmetry

Sandra Mancini [a], Sharon L. Sally [b], Rick Gurnsey [a,*]

[a] Department of Psychology, Concordia University, 7141 Sherbrooke Street West, Montréal, Qué., Canada H4B 1R6

[b] Department of Neurobiology and Anatomy, University of Rochester, 601 Elmwood Avenue, Box 603, Rochester, NY 14642, USA

Received 13 August 2003; received in revised form 18 January 2004

Abstract

To assess the role of second-order channels in symmetry perception we measured the effects of check size, spatial frequency content, eccentricity and grey scale range on the detection of symmetrical and anti-symmetrical patterns. Thresholds for symmetrical stimuli were only moderately affected by these manipulations. Anti-symmetrical stimuli composed of large black and white checks elicited low thresholds. However, anti-symmetry became essentially undetectable at small check sizes. Removing low frequencies from large-check-size, anti-symmetrical stimuli had little effect on thresholds whereas removing high frequencies had a pronounced effect. Moving the stimuli from fixation to 8° eccentricity caused a dramatic increase in thresholds for anti-symmetrical stimuli but not symmetrical stimuli. When the grey scale range was increased anti-symmetry was undetectable at any check size whereas symmetry was easily seen at all. We argue that these results and others in the literature suggest that anti-symmetry is only detected under conditions favourable to selective attention.
© 2005 Elsevier Ltd. All rights reserved.

Keywords: Polarity; Symmetry; Eccentricity; Spatial Vision; Second-order channels

1. Introduction

Bilateral-or mirror-symmetry is extremely salient to humans and has been a prominent feature of our artefacts across time and cultures. The biological significance of symmetry has been widely discussed and it has been shown that symmetry influences the behaviour of many animals, including birds and bees (e.g., Horridge, 1996; Swaddle & Cuthill, 1994). Humans are very sensitive to the presence of symmetry in images (e.g., Barlow & Reeves, 1979) and many vision scientists have speculated about the mechanisms underlying symmetry detection (see Wagemans, 1995 for a recent review). Symmetry is interesting from a signal processing point of view because it can be used to probe the nature of spatial coding mechanisms in the human visual system. The definition of bilateral symmetry provides a point of departure for posing such questions.

Points $I(x,y)$ and $I(-x,y)$ are *symmetrically placed* with respect to the y axis and an image possesses the property of *bilateral symmetry* about the y axis if

$$\forall(x,y)I(x,y) = I(-x,y). \quad (1)$$

For images satisfying Definition 1 it is clear that there is a perfect positive correlation between the intensities of points that are symmetrically placed across the y axis. From this correlational point of view, it is natural to ask whether we are equally sensitive to *anti-symmetry* defined as

$$\forall(x,y)I(x,y) = -I(-x,y). \quad (2)$$

For images satisfying Definition 2, there is a perfect negative correlation between the intensities of symmetrically placed points. Therefore, symmetrical and anti-symmetrical stimuli have the same information content. However, identical information content does not

* Corresponding author. Tel.: +1 514 848 2243; fax: +1 514 848 4545.
E-mail address: Rick.Gurnsey@concordia.ca (R. Gurnsey).

0042-6989/$ - see front matter © 2005 Elsevier Ltd. All rights reserved.
doi:10.1016/j.visres.2005.02.004

necessarily confer identical perceptual status. For example, it is well known that faces are much harder to recognize in photographic negatives than in positives even though the only difference is a polarity reversal of intensity values. If psychophysical observers are equally sensitive to symmetry and anti-symmetry they would be said to show polarity insensitivity (Tyler & Hardage, 1996). Polarity insensitivity might reveal that interesting non-linear representations contribute to symmetry detection and yield sensitivity to anti-symmetry in spite of its absence in nature and consequent lack of biological significance.

2. Sensitivity to symmetry and anti-symmetry

A number of reports have addressed the relative discriminability of symmetry and anti-symmetry (Zhang & Gerbino, 1992; Wenderoth, 1996) using relatively sparse displays comprising black and white dots on a grey background. Wenderoth's (1996) stimuli, for example, consisted of 50 dots, each subtending 0.2 degrees visual angle within a display that was about 20° in diameter. The participants' task was to discriminate randomly positioned dots from those with symmetrically positioned dots having different degrees of correlation in their intensities. Three conditions of particular interest were those referred to as MA, RA and OPP because they all contained both black and white dots. In MA stimuli, black dots matched black dots and white dots matched white dots across the axis of symmetry. Thus there was a perfect correlation between the grey-levels of symmetrically placed dots. In OPP displays there was a perfect negative correlation between the grey-levels of symmetrically placed dots; i.e., black matched white, and vice versa. In our terminology, MA stimuli are symmetrical and OPP stimuli are anti-symmetrical. For RA displays there was zero correlation in the polarity of the symmetrically placed dots; i.e., half the matches were same polarity and half were of opposite polarity. Wenderoth's (1996) data show that when averaged over all axes of symmetry tested (vertical, horizontal, left- and right-oblique), MA, OPP and RA stimuli elicited approximately 74%, 70% and 72% correct detections, respectively. Considering only the vertical axis of symmetry, MA, OPP and RA stimuli elicited approximately 80%, 82% and 81% correct detections, respectively. These results suggest that there is little relationship between discriminability and the degree of correlation across the axis of symmetry. (However, a d' analysis computed on the group data suggested a modest disadvantage for the OPP stimuli relative to MA and RA.) Similar results were reported by Saarinen and Levi (2000) who used symmetrical and anti-symmetrical stimuli comprising black and white Gaussian blobs.

Tyler and Hardage (1996) also examined the relative sensitivity to symmetry and anti-symmetry (in their terms, *same-* and *opposite-polarity* symmetry). Their stimuli comprised black and white Gaussian blobs arranged on a grey background. The blobs were either dense or sparse, and were symmetrical or anti-symmetrical about the vertical axis. The blobs were presented within two sectors either to the left and right of fixation (horizontal separations) or above and below fixation (vertical separations). Detection accuracy was measured as a function of presentation duration for several viewing distances. Sensitivity was defined as the reciprocal of the exposure duration yielding $d' = 0.5$. As viewing distance decreased, stimulus size increased and the two halves of the stimuli moved to greater eccentricities. For both symmetrical and anti-symmetrical displays performance varied little at eccentricities beyond 2° from fixation. Sensitivity to symmetry and anti-symmetry was similar in low-density displays. On average, sensitivity was higher in low density displays for both symmetry and anti-symmetry, although the effect was more pronounced in the anti-symmetry displays.

Rainville (1999) found similar sensitivities for symmetrical and anti-symmetrical patches comprising bandpass, centre-surround micropatterns. Detection accuracy was measured as a function of positional jitter added to the individual micropatterns. Accuracy declined with increasing levels of positional jitter but was generally comparable for same and opposite polarity stimuli. An exception to this trend was that detecting anti-symmetry was much more difficult than detecting symmetry in *dense* displays. Thus, Rainville's results are similar to those of Tyler and Hardage (1996).

3. Mechanisms of symmetry detection

Several recent models explain sensitivity to symmetry in terms of simple operations on the outputs of linear spatial filters (e.g., Dakin & Hess, 1997; Dakin & Watt, 1994; Gurnsey, Herbert, & Kenemy, 1998; Rainville & Kingdom, 1999, 2000, 2002). We will refer to these generally as *filtering models* because they involve multiple stages of spatial filtering. The components of these models can be explained by considering the examples of symmetry and anti-symmetry in Fig. 1(a) and (b). Panels (c) and (d) show the results of convolving (a) and (b) with a filter selective for horizontal luminance gradients and panels (e) and (f) show positive half-wave rectifications of panels (c) and (d). (A positive half-wave rectification sets all negative values in the convolution output to 0.) It is worth noting that many V1 simple cells are well described as linear filters followed by a half-wave rectification (Movshon, Thompson, & Tolhurst, 1978). Although a half-wave rectification is a non-linear operation, many computations applied to half-wave rectified

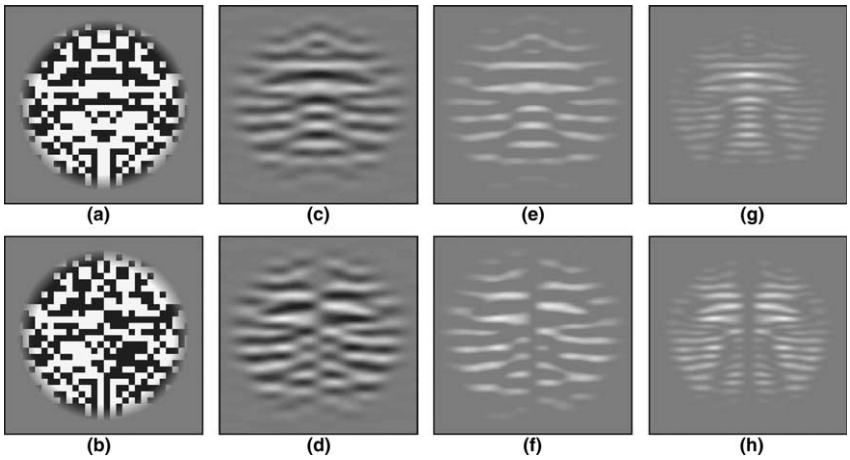

Fig. 1. Symmetrical and anti-symmetrical stimuli [(a) and (b)] that have been filtered for horizontal [(c) and (d)] and then half-wave rectified [(e) and (f)] or squared [(g) and (h)].

signals yield the same results as operations on the original (unrectified) signals. Therefore, we define the arrays of responses in panels (e) and (f) as *quasi-linear channels*.

A representation of roughly the sort shown in Fig. 1(e) forms the basis for symmetry detection in Dakin's model (Dakin & Hess, 1997; Dakin & Watt, 1994). In that model, the strength of the symmetry signal is related to the "mass" of the blobs that straddle the axis of symmetry and the degree to which their centres are aligned. The model successfully explains a number of classic results in the symmetry literature (Dakin & Watt, 1994) and new phenomena (Dakin & Herbert, 1998; Dakin & Hess, 1997). Anti-symmetry would be invisible to the model (unless a squaring or full-wave rectification is applied *prior* to initial spatial filtering). If one considers the half-wave rectification in Fig. 1(f) it is clear that no blobs straddle the axis of symmetry and hence the basis for detecting symmetrical structure is lost. In general, anti-symmetry in signals such as Fig. 1(b) cannot be detected by mechanisms that compute the equivalent of a cross-correlation across an axis of symmetry within a half-wave rectified representation such as in Fig. 1(f).

Tyler and Hardage (1996) were the first to point out that second-order channels may play an important role in symmetry detection. They argued that sensitivity to anti-symmetry and low density patterns indicates that symmetry detection is mediated predominately by second-order processes. Furthermore, because performance varied little with eccentricity (beyond 2° from fixation), these second-order processes were thought to involve connections that span the cortex.

Second-order channels are commonly created by taking the absolute value of a linear filter's response (full-wave rectification) or by squaring the filter's response (squaring rectification). V1 complex cells appear to be well described by a full-wave rectification that is achieved by summing the positive and negative half-wave rectifications of simple cell responses (Wilson, Levi, Maffei, Rovamo, & DeValois, 1990). For our purposes full-wave and squaring rectifications have similar consequences so we do not distinguish between them. Panels (g) and (h) of Fig. 1 show a squaring rectification of the linear filter responses shown in panels (c) and (d), respectively. Note that the representations in both (g) and (h) are symmetrical and may therefore provide a basis for the detection of anti-symmetry. In general, anti-symmetry in signals such as Fig. 1(b) will be detected by mechanisms that compute the equivalent of a cross-correlation across an axis of symmetry within a squaring or full-wave rectified representation such as in Fig. 1(h).

When full-wave or squaring rectifications are applied to linear filter responses the resulting representations are usually referred to as non-Fourier or *second-order channels*.[1] Second-order channels are widely used in models of related spatial tasks such as texture segmentation, motion energy extraction, and subjective contours detection, to name a few. Therefore, second-order channels may be used to achieve many computational ends.

Gurnsey et al. (1998) suggested that a differencing operation applied within quasi-linear channels would provide a basis for symmetry detection. Specifically, if the absolute response difference is computed between horizontally separated points within panels (e) or (g) then a column of zeros will form at the locus of the axis of symmetry. This "groove" could be detected by

[1] Rainville and Kingdom (2002) have a somewhat different view of Fourier and non-Fourier channels. In their model the Fourier channels produce local Fourier energy responses that are computed by summing the squared responses of bandpass, quadrature pair filters. It should be noted that their Fourier channels would yield equal sensitivity to symmetry and anti-symmetry as defined above. Their non-Fourier channel responses were computed in the same way as the Fourier channel responses but the inputs to the quadrature pair filters were the energy responses in a Fourier channel rather than the original image. So, their definition distinguishes between energy that is or is not available within the pass-band of the initial filters.

convolving the resulting representation with a filter selective for vertical. All things being equal, the magnitude of the filter's response will be related to the degree of correlation across the axis of symmetry within the representation to which it is applied. Gurnsey et al. (1998) showed that a model of this sort degrades gracefully in the presence of manipulations that are known to reduce the salience of symmetry. The model can be easily shown to yield the same sort of behaviour when presented with anti-symmetry if the differencing operation is applied in a second-order channel [Fig. 1(h)] but not when applied in a quasi-linear channel [Fig. 1(f)]. Rainville and Kingdom (2000) described a model of symmetry detection that works in much the same way as that described by Gurnsey et al. (1998) although the strategy of "groove detection" was applied to the outputs of a number of *symmetry detection units*.

The focus of the present paper is on the nature of the representations involved in the filtering mechanisms that underlie symmetry detection. We assume that if second-order channels participate in symmetry detection then equal sensitivity to symmetry and anti-symmetry would be expected. We have reviewed evidence that psychophysical subjects show roughly similar sensitivity to symmetry and anti-symmetry in sparse but not dense displays (Rainville, 1999; Tyler & Hardage, 1996; Wenderoth, 1996). Therefore, one explanation for this effect might be that sparse images activate second-order channels and dense displays activate only quasi-linear channels, leading to a loss of sensitivity to anti-symmetry.

Tyler and Hardage (1996) argued that equal sensitivity to symmetry and anti-symmetry points to the ubiquity of processes operating on second-order channels. They observed that the depth of response modulation in second-order channels decreases as density increases and used this fact to explain loss of sensitivity to anti-symmetry in dense displays.[2] In other words, anti-symmetry becomes invisible within second-order channels as density increases. [However, the simulation results of Rainville and Kingdom (2002, see Fig. 12) suggest that second-order channels should produce high sensitivity to anti-symmetry seen in even dense displays.]

It may be, however, that equal sensitivity to symmetry and anti-symmetry does not reflect the fact that they elicit similar responses from filtering models involving second-order channels. For example, it might be that sensitivity to symmetry arises from filtering models involving quasi-linear channels whereas sensitivity to anti-symmetry arises from *attentional* mechanisms that are able to operate only in sparse displays. In sparse displays there are large regions of zero contrast (homogeneous grey) and the occasional points of non-zero contrast. An attentional process might note the *symmetrical placement* of isolated tokens that differ in arbitrary ways. Attention might be the only route to detecting anti-symmetry and a second route to detecting symmetry.

Throughout this investigation we employ stimuli designed to eliminate position matching as a strategy for detecting anti-symmetry. These stimuli differ from those used by Rainville (1999), Tyler and Hardage (1996), and Wenderoth (1996) and more closely resemble those used by Jenkins (1983) and Tyler (1999). Recall that the RA stimuli used by Wenderoth (1996) involved isolated, symmetrically placed dots whose colours (black or white) were uncorrelated across the axis of symmetry, yet observers were able to detect the symmetrical structure in these displays. In contrast, all experiments reported below involve stimuli comprising densely packed checks; i.e., checks were never isolated on a grey background but completely covered the stimulus area; e.g., Fig. 1(a) and (b). In such a situation RA textures would be devoid of symmetrical structure. Thus, in the present study position alone cannot be used to convey symmetry so judgements about symmetry or anti-symmetry cannot be based solely on the symmetrical placement of individual elements.

4. Experiment 1a: the effect of check size

In Experiments 1–3, stimuli comprised black and white checks in which the proportion (p) of polarity matched checks at symmetrically placed positions varied from 1 to 0. As p increases from 0.5 to 1 the stimuli become increasingly symmetrical and as p decreases from 0.5 to 0 the stimuli become increasingly anti-symmetrical. Fig. 2 panels (a), (b) and (c) show stimuli for which $p = 1.0$, 0.75 and 0.5, respectively, and panels (d), (e) and (f) show stimuli for which $p = .0$, 0.25 and 0.5, respectively. Thresholds were defined as the proportion of polarity matched checks (p_t) required for a display to be discriminable from a random pattern (i.e., $p = 0.5$). To compare sensitivities to symmetrical and anti-symmetrical stimuli, thresholds are put on the same scale and reported as $|p_t - 0.5| + 0.5$.

In Experiment 1a thresholds were measured for symmetrical and anti-symmetrical stimuli having a range of check sizes. As check size increases, the stimuli become less dense in the sense that responses in high-frequency channels become sparser. To the extent that check size may be seen as an analogue of density in the Rainville (1999) and Tyler and Hardage (1996) studies, one might expect thresholds to decrease as a function of check size for anti-symmetrical stimuli. On the other hand, if second-order channels contribute to the coding of symme-

[2] Tyler and Hardage (1996) also point out that anti-symmetry may be detected within quasi-linear channels if the matching process can tolerate a certain amount of variability in the positions of matched items; see also Barlow and Reeves (1979) and Rainville and Kingdom (2002). We return to this in the ANALYSIS section.

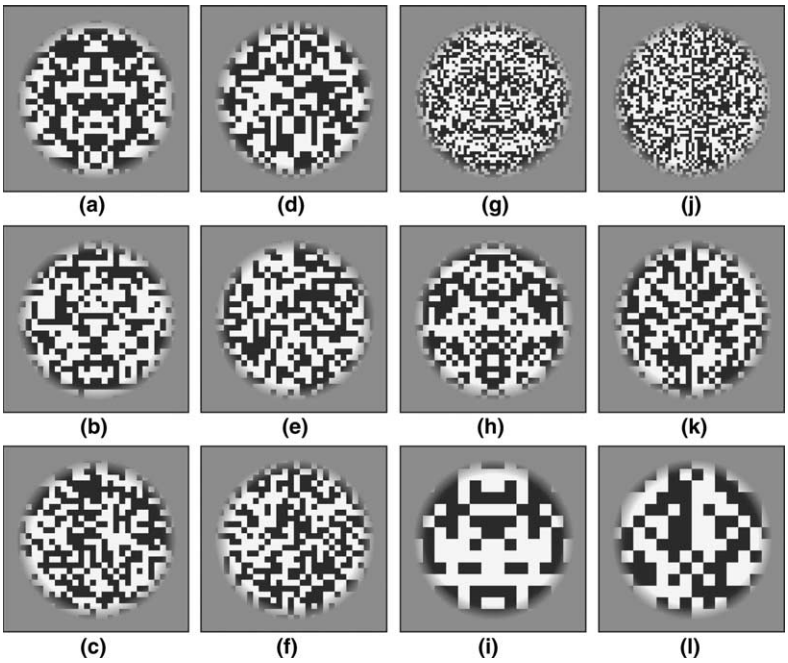

Fig. 2. Examples of stimuli with different proportions of matching elements across the vertical axis of symmetry. Pattern in the first column, top to bottom: $p = 1.0$, 0.75 and 0.5 in panels (a), (b) and (c), respectively; second column, top to bottom: $p = .0$, 0.25 and 0.5 in panels (d), (e) and (f), respectively. Examples of symmetrical (third column) and anti-symmetrical (fourth column) stimuli. From top to bottom, the check sizes are 0.148, 0.296 and 0.594 degrees of visual angle windowed within a circular aperture of 9.5 degrees in diameter.

try, then symmetrical and anti-symmetrical stimuli may elicit similar thresholds at all check sizes.

4.1. Method

4.1.1. Participants

There were five participants, three of which had extensive experience in other psychophysical tasks and the other two were novices. All had normal vision or wore the appropriate corrective lenses during the trials.

4.1.2. Apparatus

The experiments were conducted using a Macintosh G4. Stimuli were presented on a 21-inch multiscan colour monitor with display resolution set at 1024×768 pixels. Pixel width was 0.37 mm and the screen refresh rate was 85 Hz. The gamma correction software available in the Psychtoolbox (Brainard, 1997) was used to linearize the screen luminance and a Minolta CS-100 photometer was used to find the absolute luminance levels. Stimuli were created and experiments were run in the MATLAB (Mathworks Ltd.) environment using functions in the Psychtoolbox (Brainard, 1997) that provide high level access to the routines of the VideoToolbox (Pelli, 1997).

4.1.3. Stimuli

Stimuli comprised black and white checks having widths of 2, 4, 8 and 16 pixels which, from a viewing distance of 57 cm, corresponded to 0.074, 0.148, 0.296 and 0.594 degrees of visual angle. The stimuli were windowed within a circular aperture of 9.5 degrees in diameter. The third column of Fig. 2 shows examples of symmetrical stimuli ($p = 1.0$) having check sizes of 4, 8 and 16 pixels [panels (g), (h) and (i), respectively]. The fourth column of Fig. 2 shows examples of anti-symmetrical stimuli ($p = 0.0$) having check sizes of 4, 8 and 16 pixels [panels (j), (k) and (l), respectively]. The maximum and minimum stimulus luminances were 84.2 and 0.06 cd/m^2, respectively.

4.1.4. Procedure

Participants were seated 57 cm from the monitor and asked to fixate a black dot at its centre. On each trial two stimuli were presented in succession. One stimulus was completely random and the other had some degree of correlation across the axis of symmetry ($p \neq 0.5$). The task was to determine which interval contained the non-random stimulus. Stimuli were presented for 300 ms and separated by an inter-stimulus interval (ISI) of 300 ms. Therefore, the task was a two-interval forced choice (2IFC) and observers responded by clicking the mouse once or twice to indicate their choice. Visual feedback after each trial was given in the form of a "+" or "−" to indicate correct and incorrect responses. An adaptive procedure (Pentland, 1980) using a Weibull function was used to find thresholds corresponding to 82% correct detections. At least six thresholds were recorded for each observer for each of the eight conditions of the experiment. At least one threshold measurement was made

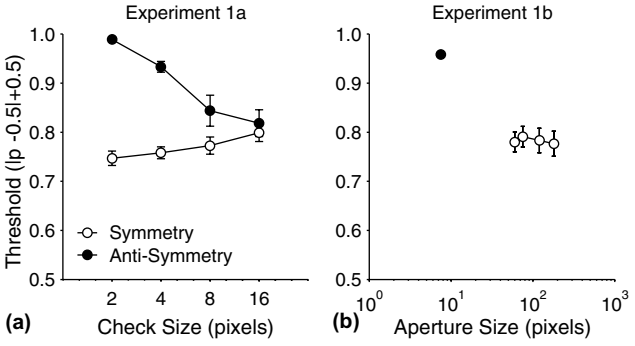

Fig. 3. (a) Threshold (±SEM) as a function of check size in pixels for symmetrical stimuli (unfilled circles) and anti-symmetrical stimuli (filled circles) ($n = 5$). The check sizes were 0.148, 0.296 and 0.594 degrees of visual angle windowed within a circular aperture of 9.5 degrees in diameter. (b) Threshold (±SEM) as a function of aperture size in pixels for symmetrical stimuli (unfilled circles) and anti-symmetrical stimuli (filled circle) ($n = 5$).

for each subject, for each experimental condition before data collection began. Thresholds for symmetry and anti-symmetry were obtained independently; i.e., symmetry and anti-symmetry trials were not interleaved.

4.2. Results

The left panel of Fig. 3 summarizes the results of Experiment 1a. We note that in many cases we were unable to obtain thresholds less than one for the anti-symmetrical stimuli. Therefore, for sessions in which PEST did not converge on a value ($|p_t - 0.5| + 0.5$) less than 1, the recorded threshold was set to 1.[3] The threshold data were submitted to a 2 (polarities) by 4 (check sizes) ANOVA. The ANOVA revealed a main effect of size [$F(3,12) = 7.5$, $p < 0.05$], a main effect of polarity [$F(1,4) = 110.2$, $p < 0.05$] and a significant interaction [$F(3,12) = 29.6$, $p < 0.05$]. The main effects of size and polarity and the size × polarity interaction explained, respectively, 65%, 96% and 88% of the variability among the means. The results show clearly different dependencies on check size for the symmetrical and anti-symmetrical stimuli. Symmetrical stimuli elicit thresholds that are relatively unaffected by check size although they do rise moderately as check size increases. Thresholds elicited by the anti-symmetrical stimuli are extremely high for the smallest check size (indeed, they are essentially unmeasurable) but drop as check size increases to a level almost identical to that elicited by the symmetrical stimuli. These results are generally consistent with those of Rainville (1999) and Tyler and Hardage (1996), if one assumes a connection between check size and density.

[3] This might be considered a questionable practice but it is clearly the lesser of two evils; taking the average of only those thresholds that converged to values less than 1 would clearly overestimate sensitivity and lead to far less representative measures of performance. This practice also leads to certain complications in the ANOVA because the sphericity assumption will be violated when the analysis includes conditions in which thresholds are uniformly high. To deal with this technical problem all reported F-tests have been subjected to the Greenhouse–Geisser correction procedure.

5. Experiment 1b: the effect of aperture size

In Experiment 1a, the size of the aperture in which stimuli were presented remained constant throughout the different check size conditions. Because this means that there were more checks within the window for the smallest sizes than for the largest, we wondered if the increase in thresholds for symmetrical stimuli was a consequence of a reduced number of checks within the aperture. Therefore, we ran further trials using symmetrical stimuli having the largest checks from Experiment 1a at a range of aperture sizes.

It is conceivable that a complimentary limitation arose in the case of the anti-symmetrical stimuli for which performance improved as check size increased. If detection of anti-symmetry actually relies on selective attention to individual checks, then this process might be overwhelmed by the large number of checks in the small-check-size conditions. To investigate this possibility, thresholds were obtained for anti-symmetrical stimuli at the smallest check size within an aperture that contained the same number of elements as for the largest check sizes in Experiment 1a.

5.1. Method

5.1.1. Participants

The participants were the same as in Experiment 1a.

5.1.2. Apparatus/procedure/stimuli

The apparatus and procedure were the same as in Experiment 1a with the following exceptions. All *symmetrical* stimuli comprised checks that were 16 pixels on a side and presented within apertures of 9.5, 11.7, 18.5, and 27.5 degrees of visual angle. The *anti-symmetrical* stimuli comprised checks that were two pixels wide and presented in an aperture that was 1.18 degrees of visual angle. Five thresholds for each of the five conditions were obtained for each of the five observers.

5.2. Results

The findings are depicted in the right panel of Fig. 3. It is clear that decreasing the aperture size for anti-symmetrical stimuli (filled circle) with the smallest check size did not improve performance; thresholds remained very close to 1 on average. It is also clear that increasing the aperture size for the large-check-size, symmetrical stimuli did not improve performance. It is reasonable to

conclude that no aperture effect was operating during Experiment 1a and that changes in performance level between symmetrical and anti-symmetrical stimuli depended on check size only.

6. Experiment 2a: high-pass filtering

The results of Experiment 1a are consistent with the previous findings of Rainville (1999) and Tyler and Hardage (1996); viz., thresholds for symmetry and anti-symmetry diverge as check size decreases. An explanation for this finding may reside in the relationship between the frequency content of the stimuli and the frequency selectivities of the mechanisms that encode symmetry and anti-symmetry. Stimuli comprising small checks have flat energy spectra, whereas those with large checks have spectra that resemble *sinc* functions; as check size increases, energy is increasingly concentrated in the low frequencies. Low thresholds for large-check-size stimuli might reveal a full-wave or squaring rectification applied to the responses of low-frequency selective spatial filters. Such a rectification would render the internal representation of an anti-symmetrical stimulus symmetrical [e.g., Fig. 1(h)]. If low thresholds for large-check-size anti-symmetrical stimuli are a consequence of a squaring rectification in low frequency channels then thresholds should increase substantially when low frequencies are removed. To evaluate this prediction we used high-pass filters to eliminate low frequencies from a subset of the stimuli used in Experiment 1a.

6.1. Method

6.1.1. Participants

Five individuals familiar with the task participated in Experiment 2a and four participated in Experiment 2b. Participants had normal vision or wore the appropriate corrective lenses during the trials.

6.1.2. Apparatus/procedure/stimuli

We measured thresholds for symmetrical and anti-symmetrical stimuli of check size 16 as well as symmetrical stimuli of check size 4. All stimuli were passed through a filter defined as

$$H = \frac{1}{1 + (c + f)^n}, \tag{3}$$

where f is frequency expressed in cycles per patch (cpp), c is the nominal cutoff frequency and n was set to 5. Cutoff frequencies of 0, 2, 4, 8, 16, and 24 cpp were used. Examples of high-passed symmetrical and anti-symmetrical stimuli are shown in the first two columns of Fig. 4. The left column shows symmetrical stimuli filtered with cutoff frequencies of 4, 8 and 16 cpp [panels (a), (b) and (c), respectively]. The second column shows

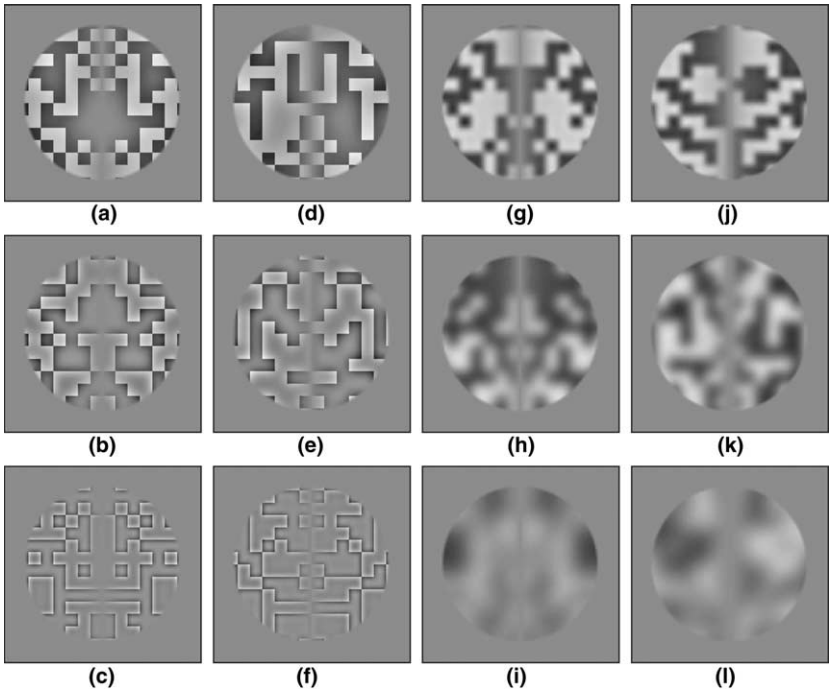

Fig. 4. Examples of high-passed filtered symmetrical (first column) and anti-symmetrical (second column) stimuli of check size 0.594 degrees of visual angle. From top to bottom, the cutoff frequencies are 4, 8 and 16 cycles/patch in panels (a)–(c) and (d)–(f), respectively. Examples of low-passed filtered symmetrical (third column) and anti-symmetrical (fourth column) stimuli of check size 0.594. From top to bottom, the cutoff frequencies are 16, 8 and 4 cycles/patch in panels (g)–(i) and (j)–(l), respectively.

anti-symmetrical stimuli filtered with cutoff frequencies of 4, 8 and 16 cpp [panels (d), (e) and (f), respectively].

Filtering produces an artefact in the anti-symmetrical stimuli that makes them easily distinguishable from filtered random noise. Specifically, filtering produces a column of zero-crossings along the *axis of anti-symmetry*; e.g., Fig. 1(h). To eliminate this *differential cue* to the presence of anti-symmetry we reduced contrast along all axes of symmetry (i.e., both symmetric, anti-symmetric and *all null stimuli*) by multiplying the signal by an inverse Gaussian weighting function

$$G = 1 - \exp(-d/\sigma), \tag{4}$$

where d is distance from the axis of symmetry and $\sigma = 8$ pixels. Once again, because all symmetric, anti-symmetric and null stimuli have reduced contrast along the axis of symmetry this cannot serve as a differential cue to the presence of anti-symmetry. Thresholds were measured as before and three replications of each condition were obtained from each participant.

6.2. Results

The results of Experiment 2a are summarized in the left panel of Fig. 5. The data were submitted to a 3 (pattern types) by 6 (filters) within subjects ANOVA. The ANOVA revealed a main effect of cutoff frequency [$F(5,20) = 9.8$, $p < 0.05$] which explained 71% of the variability in the means. This indicates a general increase in thresholds as more low frequency energy is removed from the display. Although statistically significant, the increase in thresholds from least to most filtering was at most 6%, which is quite modest in comparison to the effect of check size for anti-symmetrical stimuli, in Experiment 1a. There was also a main effect of pattern type [$F(2,8) = 18.3$, $p < 0.05$] which explained 82% of the variability among means. There was no interaction [$F(10,40) = 0.54$, $p > 0.05$] between pattern type and filtering.

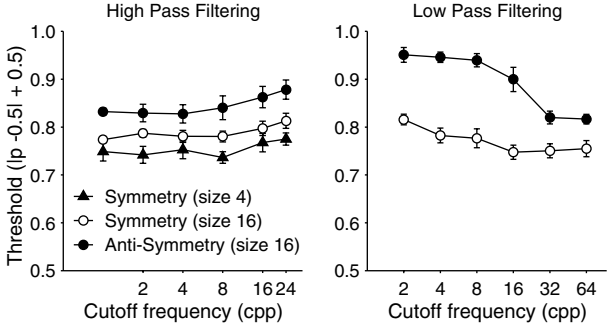

Fig. 5. (left) Threshold (±SEM) as a function of frequency cutoff for symmetrical checks of 0.148 and 0.594 degrees of visual angle and for anti-symmetrical checks of 0.594 degrees of visual angle ($n = 5$). Stimuli were passed through a high-pass filter with frequency cutoffs of 0, 2, 4, 8, 16, and 24 cycles/patch. (right) Threshold (±SEM) as a function of frequency cutoff for symmetrical and anti-symmetrical checks of 0.594 degrees of visual angle ($n = 4$). Stimuli were passed through a low-pass filter with frequency cutoffs of 2, 4, 8, 16, 32 and 64 cycles/patch.

At all levels of filtering, the symmetrical stimuli having check size 4 produced lower thresholds than symmetrical stimuli having check size 16. This is consistent with the results of Experiment 1a in which it was shown that thresholds for symmetrical stimuli decreased with decreases in check size. In contrast to Experiment 1a, thresholds were higher for anti-symmetrical stimuli having check size 16 than for symmetrical stimuli having check size 16 in the case of no filtering (see the leftmost data-points in the left panel of Fig. 5). This might suggest that participants in Experiment 1a relied on information along the vertical midline to discriminate the anti-symmetrical from random stimuli, and that reducing contrast along the vertical midline for null stimuli as well may have eliminated this cue.

The most important result of Experiment 2a is that eliminating low frequencies from large-check-size, anti-symmetrical stimuli did not lead to the dramatic increase in thresholds found in Experiment 1a when check size was reduced. In fact, there was no interaction between filtering and pattern type. This suggests that participants did not rely on the low-frequency content of the anti-symmetrical stimuli in Experiment 1a. Given the extremely modest increase in thresholds with increasingly severe high-pass filtering, it is more likely that participants relied on the high frequency content present in the anti-symmetrical displays in Experiment 1a. This possibility was addressed in Experiment 2b.

7. Experiment 2b: low-pass filtering

This experiment is identical to Experiment 2a except for the following. The stimuli were passed through a low-pass filter defined as

$$H = 1 - \frac{1}{1 + (c/f)^n}, \tag{5}$$

where f is frequency expressed in cpp, c is the nominal cutoff frequency and n was set to 5. Cutoff frequencies of 2, 4, 8, 16, 32 and 64 cpp were used.

Examples of low-passed symmetrical and anti-symmetrical stimuli are shown in the right two columns of Fig. 4.

7.1. Results

The results are summarized in the right panel of Fig. 5. The data were submitted to a 2 (polarities) × 6 (cutoff frequencies) ANOVA. The ANOVA revealed a main effect of cutoff frequency [$F(5,15) = 10.3$, $p < 0.05$] indicating a general increase in thresholds as more high frequency energy is removed, a main effect of pattern

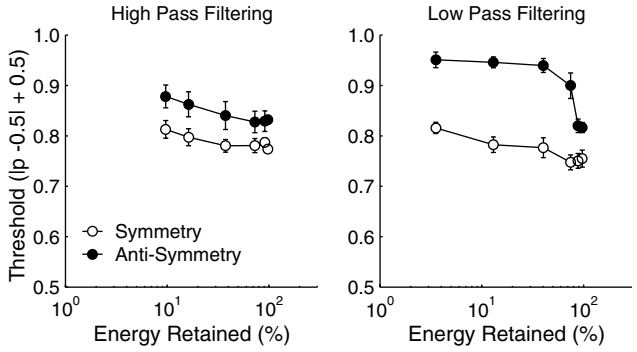

Fig. 6. Threshold (±SEM) for symmetrical and anti-symmetrical stimuli as a function of energy retained after filtering for check size 0.594 degrees of visual angle. Left ($n = 5$) and right ($n = 4$) panels represent high-, and low-pass filtered stimuli, respectively.

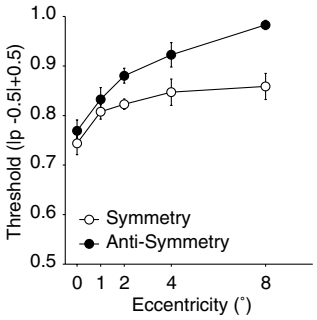

Fig. 7. Threshold (±SEM) as a function of eccentricity in degrees of visual angle for symmetrical stimuli (unfilled circles) and anti-symmetrical stimuli (filled circles) ($n = 5$). The check size was 0.594 degrees of visual angle windowed within a circular aperture of 9.5 degrees in diameter.

type [$F(1,3) = 92.2$, $p < 0.05$] with lower thresholds overall for symmetrical stimuli, and a significant interaction [$F(5,15) = 3.8$, $p < 0.05$]. The latter result reflects a more substantial increase in thresholds for anti-symmetrical than symmetrical stimuli as more high frequencies were eliminated from the displays. Cutoff frequency, polarity, and cutoff frequency × polarity explained 77%, 97% and 56% of the variability in the treatment conditions, respectively.

To facilitate a comparison of the effects of removing low and high frequencies from the displays, we have replotted in Fig. 6 the check size 16 data from the left and right panels of Fig. 5 as a function of *percent retained energy*; i.e., total stimulus energy after filtering relative to total stimulus energy before filtering. The figure shows that for symmetrical stimuli, detection performance is moderately affected by energy reductions and there is very little difference in the performance changes for reductions of high and low frequencies. For anti-symmetrical stimuli, however, performance is more seriously impaired by the loss of high frequencies than by the loss of low frequencies.

The most important result of Experiment 2b is the statistically significant interaction between polarity and cutoff frequency. This indicates that high frequencies are more important for the detection of anti-symmetry than symmetry. If the loss of high frequencies impairs the detection of anti-symmetry but not symmetry, we would expect that when symmetrical and anti-symmetrical stimuli are moved into the periphery thresholds should increase more for anti-symmetrical than symmetrical stimuli.

8. Experiment 3: eccentricity

In this experiment observers were presented with large-check-size (16 pixels) symmetrical and anti-symmetrical patterns. Thresholds were obtained at eccentricities of 0, 1, 2, 4 and 8 degrees of visual angle in the right visual field. The participants, apparatus and methodology were the same as those of Experiment 1a. Viewing was binocular.

8.1. Results

The results of Experiment 3 are summarized in Fig. 7. The data were submitted to a 2 × 5 within subjects ANOVA. The ANOVA revealed a main effect of eccentricity [$F(4,12) = 48.8$, $p < 0.05$], a main effect of polarity [$F(1,3) = 23.3$, $p < 0.05$], and a trend toward a significant interaction [$F(3,12) = 2.58$, $p = 0.09$]. The treatment effects for eccentricity, polarity and eccentricity × polarity, respectively explained 94%, 89% and 46% of the variability in the data. Fig. 7 shows that thresholds for symmetrical and anti-symmetrical stimuli were similar at fixation and clearly diverged as eccentricity increased. At 8° participants were unable to detect structure in the anti-symmetrical stimuli whereas thresholds for the symmetrical stimuli reached a plateau at $p \approx 0.86$. There is a clear parallel between Fig. 7 and the right panel of Fig. 6; in both cases as high frequencies are removed thresholds for anti-symmetry rise dramatically and those for symmetry are only modestly affected.

9. Experiment 4a: greyscale stimuli

The stimuli used in the first three experiments were intended to defeat an explicit position matching strategy for detecting anti-symmetry. It might be argued, however, that as check size increases (and check density decreases) it would be easier for subjects to explicitly compare individual checks at symmetrically placed locations to assess the probability that the 'grey-level' correlation is zero. This strategy is quite different from the idea that sensitivity to anti-symmetry arises from

filtering models involving second-order channels. It seems reasonable to assume that such an *attentional* process would also be defeated (or more severely challenged) by increasing the number of grey-levels in the display. However, it can be easily shown that filtering models involving second-order channels would not be affected by the number of grey-levels in the display. Therefore, some insight into the origins of sensitivity to anti-symmetry in large-check-size, anti-symmetrical, such as used in Experiments 1–3, might be gained by examining the effects of increasing the number of grey-levels in the stimuli.

To pursue this point we constructed symmetrical and anti-symmetrical stimuli from samples of Gaussian noise; all values greater than 3 standard deviations from the mean were clipped. A copy of each sample was reflected about the y axis and joined to the original. For anti-symmetrical stimuli, symmetrically placed elements were sign reversed, yielding a perfect negative correlation across the axis of symmetry. Performance was limited by adding random noise (drawn from the same distribution) to the symmetrical or anti-symmetrical signals. The contrasts of the signal and noise were set as follows:

$$s = \sqrt{c} * \text{signal} + \sqrt{1-c} * \text{noise} \quad (6)$$

where c is contrast (which ranges for 0 to 1) and signal and noise represent the symmetrical (or anti-symmetrical) image and noise component of the display, respectively. The signals were then quantized to 254 grey levels for presentation on the computer monitor.

9.1. Method

9.1.1. Participants

Five individuals participated in all conditions. All were experienced psychophysical observers and all had normal vision or wore the appropriate corrective lenses during the trials.

9.1.2. Apparatus/procedure/stimuli

Symmetrical and anti-symmetrical displays were created with check-sizes of 2, 4, 8 and 16 pixels. Examples of the stimuli are presented in Fig. 8. The left column [(a)–(c)] shows symmetrical stimuli with $c = 1$. The second column [(d)–(f)] shows symmetrical stimuli with $c = 0.8$. The third column [(g)–(i)] shows anti-symmetrical stimuli with $c = 1$ and the fourth column [(j)–(l)] shows anti-symmetrical stimuli with $c = 0.8$. Although the patterns in columns 1 and 3 are set to full contrast ($c = 1$) and those in columns 2 and 4 have $c = 0.8$, to most observers all patterns in columns 1 and 2 appear symmetrical whereas those in columns 3 and 4 appear random.

The apparatus and procedure were exactly as in Experiment 1a, with the following exceptions. The PEST procedure was replaced by the QUEST procedure (Watson & Pelli, 1983) and stimulus contrast (c) was

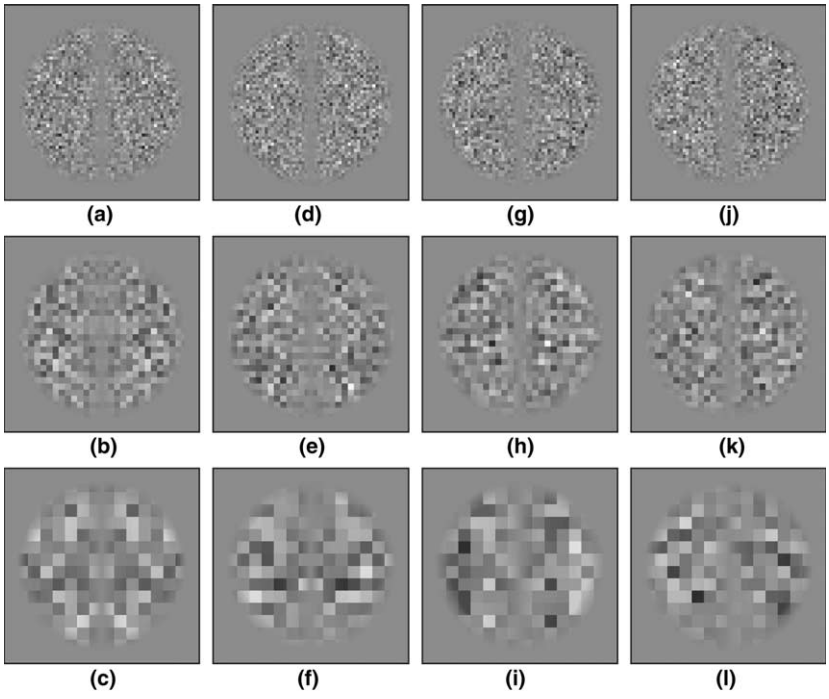

Fig. 8. Examples of symmetrical [(a)–(f)] and anti-symmetrical [(g)–(l)] greyscale stimuli. The first and third columns were stimuli with $c = 1$ and second and fourth columns were stimuli with $c = 0.8$. From top to bottom, the check sizes are 0.148, 0.296 and 0.594 degrees of visual angle windowed within a circular aperture of 9.5 degrees in diameter.

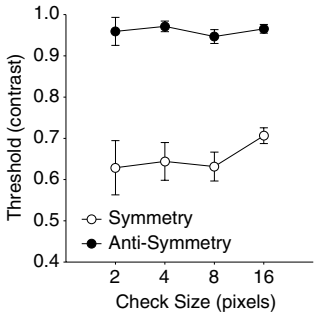

Fig. 9. Contrast thresholds (±SEM) as a function of check size in pixels for symmetrical stimuli (unfilled circles) and anti-symmetrical stimuli (filled circles) ($n = 5$).

varied rather than the proportion of matching elements.[4] Three thresholds were obtained in each of the eight conditions for four of the five participants, and one replication was obtained for the remaining participant.

9.2. Results

The results are summarized in Fig. 9. The data were submitted to a 2 (polarities) × 4 (check size) within participants ANOVA. The ANOVA revealed a main effect of polarity [$F(1,4) = 142.7$, $p < 0.05$] but no main effect of check size [$F(3,12) = 0.71$, $p > 0.05$] and no interaction [$F(3,12) = 1.26$, $p > 0.05$]. Polarity explained 97.2% of the variability in the data.

The results in Fig. 9 are very different than those in the left panel of Fig. 3. The principal difference is that thresholds for anti-symmetrical stimuli do not drop for large check sizes in Fig. 9 as they do in the left panel of Fig. 3. These results suggest that the ease with which large check size, anti-symmetrical stimuli were detected in Experiment 1a has something to do with the limited number of grey levels rather than with a general second-order rectification process.

10. Experiment 4b: binary and greyscale stimuli

Although a comparison of Experiments 4a and 1a suggests that sensitivity to anti-symmetry is very different in the two conditions, it could be objected that there are many differences between the two experiments that might contribute to the observed differences. For example, Experiment 1a used binary stimuli, the PEST procedure and varied proportion of matching checks to control performance, whereas Experiment 4a used grey-scale stimuli, the QUEST procedure, varied stimulus and noise contrast to limit performance, and reduced the contrast along the axis of symmetry (as in Experiment 2). Experiment 4b was conducted to assess the relative salience of binary and greyscale stimuli under more similar conditions.

The greyscale stimuli were essentially as shown in Fig. 8 except that contrast was not reduced along the axis of symmetry. Binary stimuli were created exactly as were the greyscale stimuli except that in an added step the grey-levels were made binary by setting intensities greater than the mean to white and those less than the mean to black. This manipulation produces a continuous variation in the strength of the symmetry and anti-symmetry signals; i.e., it accomplishes essentially the same thing as the "proportion matching" manipulation used in Experiments 1–3, but in a slightly different way. In both cases thresholds were obtained using the QUEST procedure.

10.1. Method

10.1.1. Participants

Five individuals participated in all conditions. All were experienced psychophysical observers and all had normal vision or wore the appropriate corrective lenses during the trials.

10.1.2. Apparatus/procedure/stimuli

Except for the changes in stimuli described above, all aspects of the procedure were as described in Experiment 4a. Two to four thresholds were obtained in each condition for each participant.

10.2. Results

The results are summarized in Fig. 10. The main points can be made by noting that the left panel of Fig. 10 is essentially identical to the left panel of Fig.

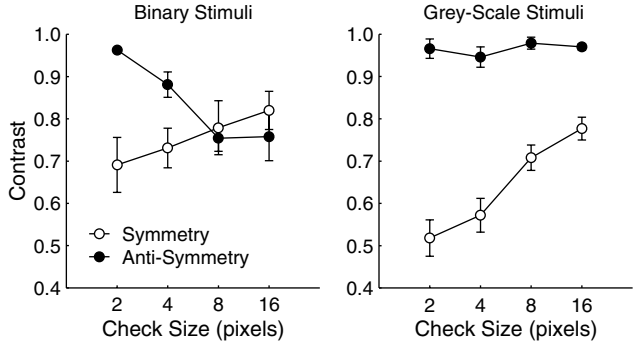

Fig. 10. Contrast thresholds (±SEM) as a function of check size in pixels for symmetrical stimuli (unfilled circles) and anti-symmetrical stimuli (filled circles) for both binary (left, $n = 5$) and greyscale (right, $n = 5$) conditions.

[4] When dealing with binary stimuli it makes sense to talk about "proportion of matching elements" whereas it is not as obvious what should constitute a match given that each check may take on one of 254 different grey-levels.

3 indicating that the interaction between polarity and check size does not depend on the method used to degrade symmetry and anti-symmetry. As well, the right panel of Fig. 10 is essentially identical to Fig. 9, indicating that the results are little affected by the presence or absence of the contrast reduction along the axis of symmetry.

11. Analysis

The results of Experiments 2 and 3 suggest that detecting anti-symmetry requires the presence of high frequencies and the results of Experiments 1a and 2a suggest that the responses of high frequency selective filters must be relatively sparse. These results cannot be explained by a squaring rectification (or energy computation) in high frequency channels followed by a precise matching procedure.[5] Although this kind of procedure would produce good performance in large check size, anti-symmetrical displays, it can be easily shown that it would produce even better performance in small check size, anti-symmetrical displays and this would be inconsistent with the results of Experiment 1a. A half-wave rectification followed by a precise matching procedure cannot explain the pattern of results. Again, it can be easily shown that such a procedure would produce poor performance for all anti-symmetrical displays and this would be inconsistent with the results of Experiments 1a, 2a and 3. The low thresholds for large-check-size, anti-symmetrical stimuli in Experiments 1a, 2a and 3 might be explained by *imprecise matching* in a quasi-linear channel.

Passing anti-symmetrical displays through an isotropic, zero-mean, bandpass filter produces responses that are phase reversed on either side of zero crossings. In Fig. 4f, for example, symmetrically placed filter responses are sparse and sign reversed on either side of zero-crossings. If this representation (Fig. 4f) were half-wave rectified, then an imprecise matching procedure might note the high correlation in activity in roughly symmetrical positions. Furthermore, as suggested by Tyler and Hardage (1996) such a process might be defeated as check size decreases because there would be many more candidate matches within any region. This would increase the chances of false matches occurring and result in reduced sensitivity. Increasing the number of grey-levels in a display might also disrupt an imprecise matching strategy. The results of Experiments 4a and b might be seen to support this qualitative account. Therefore, it is possible that all the data in Fig. 10 could be explained by a filtering model that somehow embodies imprecise matching within quasi-linear channels.

To assess this hypothesis we implemented a simple computational model of symmetry detection. The model consisted of filtering with a $\nabla^2 G$ filter (Marr & Hildreth, 1980), a half-wave rectification followed by Gaussian blurring which in turn was followed by cross-correlation to assess symmetry. The $\nabla^2 G$ filter is defined as

$$\nabla^2 G(r,\sigma) = 1/\pi^4 \left(1 - \frac{r^2}{\sigma^2}\right) e^{-(r^2/2\sigma^2)} \quad (7)$$

where r is the distance from the centre of the window and s, the spread of the Gaussian component of the filter, was set to 0.75 pixels, which made it sensitive to about 60 cpp (corresponding to about 6.3 cpd in terms of the displays used in the experiments). We chose a filter tuned to high spatial frequencies for two reasons. First, the results of Experiment 2 suggested that detection of large-check-size, *anti-symmetrical* stimuli requires the presence of high frequencies. Second, *symmetry* detection at all check sizes was not severely impaired by the elimination of low frequencies. The half-wave rectifier set all negative values in the convolution output to 0, thus yielding a quasi-linear channel as defined in Section 1.

The imprecise matching was accomplished by blurring the rectified response with an isotropic Gaussian filter. The use of Gaussian blurring to model imprecise matching follows from the observations of Barlow and Reeves (1979) that slight perturbations of dot positions in random dot, symmetrical displays had little effect on human performance but completely defeated an ideal observer that computed correlations at symmetrical positions. Barlow and Reeves pointed out that if the image were blurred before correlations were computed the performance of the ideal observed could be substantially improved. In a similar manner, an ideal observer that uses precise positional information would not be able to detect anti-symmetry in any half-wave rectified representation. However, if the half-wave rectified representation is blurred, then the correlation in activity at symmetrically positioned points will increase.

The question now is whether the pattern of results in Fig. 10 can be captured by the model. Three versions of the model were evaluated, each differing only in the spread of the Gaussian blurring applied to the quasi-linear channel. The three Gaussian kernels had σ's of 1, 2 and 4 pixels. The stimuli were identical in all respects to those used in Experiment 4b except that they were scaled to 50% of the original size. The conditions tested were exactly the 16 cells of Experiment 4b; i.e., 4 check sizes (1, 2, 4 and 8) × 2 display types (symmetry vs. anti-symmetry) × 2 grey-scales ranges (2 vs. 254) = 16.

[5] For simplicity, in this section we do not consider specific models of symmetry detection. Rather we consider the information available within quasi-linear and second-order channels and their variants. We use cross-correlation to assess this information. The *precise-* and *imprecise matching* terminology arises from this correlational perspective.

On each simulated trial a stimulus display having some non-zero contrast (c) and a null stimulus ($c = 0$) were submitted to the model. For both displays the cross-correlation across the axis of symmetry was computed and the one that produced the largest cross-correlation was chosen as symmetric. Thresholds were found using the QUEST procedure exactly as in Experiment 4a. Ten thresholds were obtained for each of the 16 cells, for each of the three models.

The simulation results are shown in Fig. 11. The left and right panels shows results for binary and greyscale stimuli, respectively. Unfilled symbols indicate symmetrical displays and filled symbols indicate anti-symmetrical displays. The three degrees of post-rectification blurring are indicated by circles, squares and triangles for σ's 1, 2 and 4, respectively. There are three important observations to be made. First, as blurring increases, thresholds decrease for anti-symmetrical stimuli and increase for symmetrical stimuli. This apparently paradoxical result is easily explained by the effects that blurring has on the target displays (symmetrical and anti-symmetrical) and null displays. Reduced thresholds for anti-symmetrical displays are attributable to the increased correlation across the axis of symmetry that arises from blurring; i.e., blurring produces the expected result. On the other hand, blurring also increases the correlation across the axis of symmetry for null displays. Consequently, contrast in the symmetrical image must be increased to exceed the blur induced correlations in the null displays.

Second there is little evidence that thresholds decrease for anti-symmetrical stimuli as check size increases for any of the levels of blurring. To the contrary, for $\sigma = 2$ and 4 thresholds for anti-symmetrical stimuli increase with check size. It might be objected, however, that our model of symmetry detection is not realistic in that decisions are based on the magnitudes of cross-correlations (e.g., Dakin & Hess, 1997; Dakin & Watt, 1994) rather than on a biologically plausible mechanism of symmetry detection (e.g., Gurnsey et al., 1998; Rainville & Kingdom, 1999, 2000, 2002). If such models were studied in conjunction with the assumption that performance is limited by internal noise then it might be that an appropriate level of internal noise would yield the pattern of results seen in the left panels of Figs. 3 and 10.

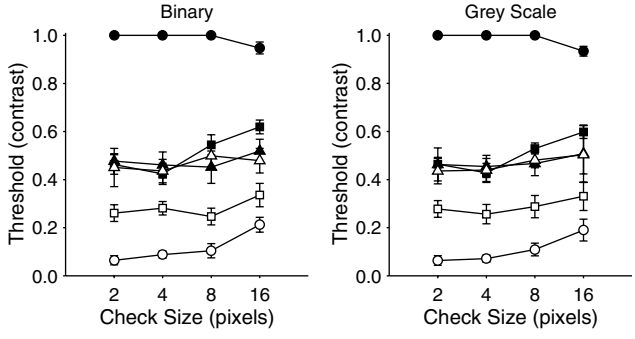

Fig. 11. Simulated thresholds for binary (left) and greyscale stimuli (right), symmetrical (unfilled symbols) and anti-symmetrical (filled symbols) stimuli. Three degrees of post-rectification blurring (σ's = 1, 2 and 4 pixels) are shown as circles, squares and triangles, respectively.

However, our final point is that the simulation results in the left and right panels of Fig. 11 are identical. That is, even if introducing internal noise into a biologically plausible model were sufficient to capture the pattern of results in the left panels of Figs. 3 and 10 (i.e., binary stimuli) exactly the same pattern of results would be produced for the greyscale stimuli (right panel of Fig. 10). We conclude that an imprecise matching procedure applied within a high-frequency, quasi-linear channel can improve sensitivity to anti-symmetry. However, such a strategy would produce similar thresholds for binary and greyscale stimuli and this result is contradicted by the psychophysical data.

12. General discussion

12.1. Symmetry vs. anti-symmetry

A review of the literature showed that symmetrical and anti-symmetrical stimuli elicit comparable performance when composed of isolated tokens separated by regions of intermediate grey (Rainville, 1999; Saarinen & Levi, 2000; Tyler & Hardage, 1996; Wenderoth, 1996) and when tokens are sampled from binary distributions such as black and white dots (Wenderoth, 1996), black and white Gaussian blobs (Saarinen & Levi, 2000; Tyler & Hardage, 1996) or centre-surround elements of opposite polarity (Rainville, 1999). Tyler and Hardage explained sensitivity to such anti-symmetries in terms of second-order channels (see also Rainville, 1999). Experiment 1a generally replicated the results of Tyler and Hardage; thresholds for symmetry and anti-symmetry were similar in binary displays comprising large checks but diverged as check size decreased. This result might be seen as consistent with a role for second-order channels in symmetry perception. However, Experiment 4 showed that anti-symmetry was undetectable even in displays comprising large checks when the grey scale range of the checks was increased. This result is inconsistent with the idea that second-order channels generally play an important role in symmetry detection.

Our experiments show that thresholds for symmetrical stimuli were only modestly affected by manipulations of check size, spatial frequency content, eccentricity and greyscale range. It seems reasonable, therefore, to posit the existence of linear or quasi-linear channels that support sensitivity to symmetry. Such channels might operate as described by Gurnsey et al. (1998) or Rainville and Kingdom (2000) and take a half-wave rectified

signal as input. Assuming the entire mechanism integrates information across scales (Rainville & Kingdom, 1999) it is easy to understand why eliminating some spatial frequency information through explicit filtering (Experiment 2) or by moving the stimulus into the periphery (Experiment 3) would lead to modest increases in thresholds. It can also be shown that increasing check size reduces information density (Rainville & Kingdom, 2000) which leads to modest threshold increases (Experiments 1 and 4).

Assuming the existence of a second-order channel to accommodate a subset of the present results predicts sensitivities that are inconsistent with other results reported here. For example, positing the availability of low frequency, second-order channels to explain low thresholds for large-check-size, anti-symmetrical stimuli in Experiment 1a is inconsistent with the effects of filtering in Experiment 2 and the complete insensitivity to large-check-size, anti-symmetrical greyscale stimuli in Experiment 4.

Our results do not imply that second-order channels never contribute the the detection of symmetry and anti-symmetry. For example, there are many differences between our experimental methodology and that of Tyler and Hardage (1996), which yielded equivalent sensitivity to symmetry and anti-symmetry. Therefore, determining the conditions under which second-order channels make a contribution to symmetry detection requires further study. However, it seems that second-order channels make little if any contribution to symmetry detection under the conditions of the present experiments. In fact, the results suggest two kinds of processes available for the detection of symmetry and anti-symmetry. One type of process has access to first-order channels and is able to match information across the axis of symmetry; such a process might have the character of the mechanisms described by Dakin and Watt (1994), Gurnsey et al. (1998) or Rainville and Kingdom (2002). When first-order information is unavailable this process fails. For example, in high density displays subjects are very sensitive to symmetry conveyed by first-order information but if the first-order information is removed, by making the display anti-symmetrical, then detection becomes impossible, at least under the conditions of our experiments.

A second process is revealed by the fact that anti-symmetry is detected when items are sparsely distributed on a neutral background (Rainville, 1999; Tyler & Hardage, 1996; Wenderoth, 1996). We suggest that a second route to the detection of symmetry and anti-symmetry involves an explicit assessment of token position (independently of their colour) when density is low (Rainville, 1999; Tyler & Hardage, 1996; Wenderoth, 1996). When density increases this strategy becomes ineffective because there are too many positions to consider in the time available. Furthermore, in displays such as ours detection of anti-symmetry (and symmetry for that matter) might be achieved by combining information about position and colour when there are few items in the display [e.g., Fig. 2(l)]. Specifically, it may be possible to compare symmetrical locations, note their colours and assess the probability that there is zero correlation between colour and position across the axis of symmetry. However, such a process would be defeated if either the number of locations to compare is too great (i.e., small-check-size displays), or if fine discriminations between grey-levels are required (e.g., the greyscale stimuli used in Experiment 4). Because this second strategy seems to operate in conditions that favour selective attention, we assume that it is not low-level in the sense of the models described by Dakin and Watt (1994), Gurnsey et al. (1998), Rainville and Kingdom (1999, 2000, 2002) or Tyler and Hardage (1996).

There are a number of paradigms that could be used to assess whether detection of anti-symmetry differs from detection of symmetry in its reliance of attentional resources. One might be to assess the susceptibility of symmetry and anti-symmetry detection to attentional manipulations. For example, participants could be asked to perform a second, resource demanding task while trying to detect symmetry or anti-symmetry (Braun & Julesz, 1998). The dual route proposal suggests that anti-symmetry detection might be more impaired by this manipulation than symmetry detection. The effects of invalid, exogenous 'cuing' might be assessed in a similar way. The appearance of an invalid exogenous cue prior to the presentation of a symmetrical or anti-symmetrical display might draw certain resources away from the patterns and the consequence might be greater disruption of anti-symmetry detection than symmetry detection.

12.2. Frequency content

The effects of frequency manipulation in Experiment 2 may be compared to the results of Rainville and Kingdom (1999). They created symmetrical patterns from white noise to which was added uncorrelated white noise (much as in Experiment 4). The resulting patterns (which had flat spectra) were then filtered to have $1/f^{\beta}$ spectra for b ranging from -2 to 5. When $\beta = 0$ stimuli have flat spectra, when $\beta < 0$ there is high frequency emphasis and when $\beta > 0$ there is low frequency emphasis. Natural images are found to have spectral slopes in the range $1.2 \leqslant \beta \leqslant 3.2$. Rainville and Kingdom (1999) wondered if there might be an advantage for symmetry detection for slopes in this range. To answer this they varied the signal-to-noise ratio to find threshold (81% correct responses in a 2AFC task). As expected, thresh-

olds show a U shaped dependence on β, with lowest thresholds in the range associated with natural images.

We found a similar result. When combining the results of Experiments 2a and b, for large-check-size symmetrical stimuli, we find a U shaped dependence on spatial frequency content (i.e., concatenate the unfilled circles in the right panel of Fig. 5 with the unfilled circles in the left panel of Fig. 5). The unfiltered stimuli in this case have spectra that resemble *sinc* functions with energy concentrated around the origin. Thus, the spectra of our unfiltered, large-check-size stimuli are more similar to $\beta > 0$ spectra than $\beta < 0$ spectra. Removing high or low frequencies increased thresholds, although as stated the increases were rather modest. It is difficult to compare directly the results of Rainville and Kingdom's (1999) study with ours because the psychometric variables were different. They varied signal-to-noise ratio, which ranged from 0 to 1 and we varied percent matching, which ranged from 0.5 to 1. When the thresholds from the two studies are expressed as a proportion of the range of the variable, the largest average difference in their data was about 0.24 and in ours about 0.13. Therefore, the consequences of spectral manipulations were generally greater in their experiment than in ours. These comparisons should be treated with caution, however, because of the significant differences in the way that performance was measured.

The results of Experiments 2a and b suggest that symmetry is computed simultaneously at several scales; i.e., within several spatial frequency channels. For symmetrical stimuli we found comparable thresholds for stimuli having radically different spectra (i.e., low passed and high passed stimuli with cut-offs differing by more than 3.5 octaves). These results are consistent with those of Rainville and Kingdom (1999, Experiment 2) who provide additional evidence for the idea that symmetry calculations are performed in parallel at several different scales.

12.3. Eccentricity

Several recent studies have examined the effects of eccentricity on symmetry detection (Barrett, Whitaker, McGraw, & Herbert, 1999; Gurnsey et al., 1998; Sally & Gurnsey, 2001; Tyler, 1999; Tyler & Hardage, 1996). Three of these studies show reduced sensitivity to symmetrical stimuli of fixed size as they are moved into the periphery (Barrett et al., 1999; Gurnsey et al., 1998; Sally & Gurnsey, 2001). Although the experiments differ in detail they converge on the conclusion that stimuli must be magnified substantially with eccentricity to achieve equivalent-to-foveal performance.

On the other hand, Tyler (1999) reported that peak sensitivity to stimuli of fixed size does not change substantially with eccentricity. Again, sensitivity was defined by the exposure duration required to elicit a d' of 0.5. Our results for symmetrical stimuli seem to fall between these two patterns. We found an initial increase in thresholds as stimuli were moved from fixation to 2° and thereafter reached an asymptote. Of course a nonlinear relationship between 'percent-matching' thresholds and eccentricity is to be expected, so care must be taken when interpreting this result. In fact, it would be worthwhile to measure percent-matching thresholds for both symmetrical and anti-symmetrical stimuli over a range of stimulus sizes and eccentricities to determine the scaling required to elicit equivalent performance across the visual field (Barrett et al., 1999; Sally & Gurnsey, 2001). Our results suggest that much steeper scaling would be required for anti-symmetrical stimuli than for symmetrical stimuli.

13. Conclusions

The results reported here strongly suggest that under the present experimental conditions sensitivity to symmetry and anti-symmetry does not generally arise from similar mechanisms. Thresholds for the detection of symmetry and anti-symmetry diverge as a function of check size, spatial frequency content, greyscale range and eccentricity. Thresholds for symmetry detection are relatively unaffected by any of our manipulations and this suggests the existence of low-level mechanisms that are prepared to detect symmetry at a range of scales. We find that anti-symmetry is only detected when there are few items in the display and these items have binary grey levels. These conditions suggest the need to compare individual items in the display, and hence the involvement of selective attention.

Acknowledgment

This research was supported by NSERC and FCAR Research Grants to Rick Gurnsey. Portions of this paper were presented at the ARVO annual meeting, 2001, Fort Lauderdale, Florida, and the Vision Science Society annual meetings, 2002, 2003, Sarasota, Florida.

References

Barrett, B. T., Whitaker, D., McGraw, P. V., & Herbert, A. M. (1999). Discriminating mirror symmetry in foveal and extra-foveal vision. *Vision Research, 39*, 3737–3744.

Barlow, H. B., & Reeves, B. C. (1979). The versatility and absolute efficiency of detecting mirror symmetry in random dot displays. *Vision Research, 19*, 783–793.

Brainard, D. H. (1997). The psychophysics toolbox. *Spatial Vision, 10*, 443–446.

Braun, J., & Julesz, B. (1998). Withdrawing attention at little or no cost: Detection and discrimination tasks. *Perception & Psychophysics, 60*, 1–23.

Dakin, S. C., & Herbert, A. M. (1998). The spatial region of integration for visual symmetry detection. *Proceedings of the Royal Society of London B., 265*(1397), 659–664.

Dakin, S. C., & Hess, R. F. (1997). The spatial mechanisms mediating symmetry perception. *Vision Research, 37*, 2915–2930.

Dakin, S. C., & Watt, R. J. (1994). Detection of bilateral symmetry using spatial filters. *Spatial Vision, 8*, 393–413.

Gurnsey, R., Herbert, A. M., & Kenemy, J. (1998). Bilateral symmetry embedded in noise is detected accurately only at fixation. *Vision Research, 38*, 3795–3803.

Horridge, G. A. (1996). The honeybee (apis mellifera) detects bilateral symmetry and discriminates its axis. *Journal of Insect Physiology, 42*, 755–764.

Jenkins, B. (1983). Redundancy in the perception of bilateral symmetry in dot textures. *Perception & Psychophysics, 32*, 171–177.

Marr, D., & Hildreth, E. (1980). Theory of edge detection. *Proceedings of the Royal Society of London B., 207*, 187–217.

Movshon, J. A., Thompson, I. D., & Tolhurst, D. J. (1978). Spatial summation in the receptive fields of simple cells in the cat's striate cortex. *Journal of Physiology, 283*, 53–77.

Pelli, D. G. (1997). The VideoToolbox software for visual psychophysics: Transforming numbers into movies. *Spatial Vision, 10*, 437–442.

Pentland, A. (1980). Maximum likelihood estimation: The best PEST. *Perception & Psychophysics, 28*, 377–379.

Rainville, S. J. M. (1999). *The spatial mechanisms mediating the perception of mirror symmetry in human vision*. Ph.D. Thesis. McGill University, Montreal, Quebec, Canada, Unpublished.

Rainville, S. J. M., & Kingdom, F. A. A. (1999). Spatial-scale contribution to the detection of mirror symmetry in fractal noise. *Journal of the Optical Society of America A, 16*, 2112–2123.

Rainville, S. J. M., & Kingdom, F. A. A. (2000). The functional role of oriented spatial filters in the perception of mirror symmetry-psychophysics and modeling. *Vision Research, 40*, 2621–2644.

Rainville, S. J. M., & Kingdom, F. A. A. (2002). Scale invariance is driven by stimulus density. *Vision Research, 42*, 351–367.

Saarinen, J., & Levi, D. M. (2000). Perception of mirror symmetry reveals long-range interactions between orientation-selective cortical filters. *Neuroreport, 11*, 2133–2138.

Sally, S. L., & Gurnsey, R. (2001). Symmetry detection across the visual field. *Spatial Vision*, 217–234.

Swaddle, J. P., & Cuthill, I. C. (1994). Preference for symmetric males by female zebra finches. *Nature, 367*, 165–166.

Tyler, C. W. (1999). Human symmetry detection exhibits reverse eccentricity scaling. *Visual Neuroscience, 16*, 919–922.

Tyler, C. W., & Hardage, L. (1996). Mirror symmetry detection: Predominance of second-order pattern processing throughout the visual field. *Human Symmetry Perception*, 157–171.

Wagemans, J. (1995). Detection of visual symmetries. *Spatial Vision, 9*, 9–32.

Watson, A. B., & Pelli, D. G. (1983). QUEST: A Bayesian adaptive psychometric method. *Perception & Psychophysics, 33*, 113–120.

Wenderoth, P. (1996). The effects of the contrast polarity of dot-pair partners on the detection of bilateral symmetry. *Perception, 25*, 757–771.

Wilson, H. R., Levi, D., Maffei, L., Rovamo, J., & DeValois, R. (1990). The perception of form: Retina to striate cortex. In L. Spillmann & J. S. Werner (Eds.), *Visual perception: the neurophysiological foundations* (pp. 231–271). San Diego, CA: Academic Press Inc.

Zhang, L., & Gerbino, W. (1992). Symmetry in opposite-constrast dot patterns. *Perception, 21*(Suppl. 2), 95.